Reaction limited aggregation in surfactant-mediated epitaxy

Jing Wu and Bang-Gui Liu
Institute of Physics & Center of Condensed Matter Physics, Chinese Academy of Sciences, P.O. Box 603, Beijing 100080, People's Republic of China

Zhenyu Zhang
Solid State Division, Oak Ridge National Laboratory, Oak Ridge, Tennessee 37831-6032 and Department of Physics, University of Tennessee, Knoxville, Tennessee 37996

E. G. Wang
Institute of Physics & Center of Condensed Matter Physics, Chinese Academy of Sciences, P.O. Box 603, Beijing 100080, People's Republic of China
(Received 29 September 1999)

A theoretical model for reaction limited aggregation (RLA) is introduced to study the effect of a monolayer of surfactant on the formation of two-dimensional islands in heteroepitaxial and homoepitaxial growth. In this model the basic atomic processes are considered as follows. A stable island consists of the adatoms that have exchanged positions with the surfactant atoms beneath them. Movable active adatoms may (a) diffuse on the surfactant terrace, (b) exchange positions with the surfactant atoms beneath them and become island seeds (seed exchange), or (c) stick to stable islands and become stuck but still active adatoms. The rate-limiting step for the formation of a stable island is the seed exchange. Furthermore, a stuck but still active adatom must overcome a sizable potential-energy barrier to exchange positions with the surfactant atom beneath it and become a member of the stable island (aided exchange). The seed exchange process can occur with an adatom or collectively with an addimer. In the case of dimer exchange, the diffusing adatoms on the surfactant terrace can meet and (after exchanging) form stable dimers, which can then become island seeds. Systematic kinetic Monte Carlo simulations and rate-equation analysis of the model are carried out. The key finding of these simulations is that a counterintuitive fractal-to-compact island shape transition can be induced either by *increasing* deposition flux or by *decreasing* growth temperature. This major qualitative conclusion is valid for both the monomer and the dimer seed exchanges and for two different substrate lattices (square and triangular, respectively), although there are some quantitative differences in the flux and temperature dependence of the island density. The shape transition observed is contrary to the prediction of the classic diffusion-limited aggregation (DLA) theory, but in excellent qualitative agreement with recent experiments. In rationalizing the main finding, it is crucial to realize that the adatoms stuck to a stable island edge are still active and are surrounded by the surfactant atoms. Therefore, these stuck atoms cannot capture incoming adatoms before they join the island through aided exchange. As a result, an incoming adatom must on average hit the island many times before it finally finds a free edge site to stick to. This search is effectively equivalent to edge diffusion in DLA theory. The stuck adatoms thus act as shields which prevent other mobile adatoms from sticking to the stable islands. This shielding effect, determined by the aided exchange barrier and the density of the mobile adatoms, plays an essential role in inducing the above shape transition in surfactant-mediated epitaxial growth.

I. INTRODUCTION

In heteroepitaxial growth the presence of strain often leads to three-dimensional (3D) growth, resulting in the formation of rough films. An important development in trying to overcome this fundamental obstacle was reported in 1989 when Copel *et al.*[1] demonstrated that the use of a monolayer of As can induce layer-by-layer growth of Ge on Si at much higher Ge coverage. This remarkable behavior was termed as the surfactant effect. Since then, many surfactants have been successfully used to modify the growth modes during homoepitaxial and heteroepitaxial growth in both metal[2–4] and semiconductor[5–7] systems, and a large number of experimental and theoretical studies have been devoted to understanding the fundamental mechanisms involved in surfactant action.[8] However, most of these studies, either experimental[2–7,9] or theoretical,[10–16] have concentrated on how the surfactant changes the growth mode from 3D to layer-by-layer (LBL) or Frank–van der Merwe growth. Little effort has been made to understand the pattern formation of the two-dimensional (2D) islands formed in the early stages of surfactant mediated growth, although it is believed that the morphology and the distribution of the 2D islands formed at submonolayer coverage have a significant influence on the growth mode in the multilayer regime.

The scanning tunneling microscopy (STM) is a powerful method to characterize such islands at the atomic scale. Using this technique, it has been established that islands become more fractal-like when the growth temperature is decreased at a given deposition flux, or when the deposition

flux is increased at a given growth temperature.[17–22] This can be explained by the classic ''hit-stick-relax'' scenario of the diffusion-limited aggregation (DLA) theory.[23] During real growth, the deposited adatoms are randomly and continuously deposited on the surface, and an adatom reaching an island will attempt to relax locally in order to find an energetically more favorable configuration. If the adatoms have sufficient time to relax locally along the island edges, a compact island will be obtained, otherwise a fractal island will be formed. The transition from a fractal to a compact island therefore occurs when the degree of local relaxation increases (either through an increase in the growth temperature or through a decrease in the deposition flux).[24–26]

These earlier studies on the 2D pattern formation, however, have focused on the epitaxial growth of systems without a surfactant. The presence of a surfactant obviously modifies the microscopic growth processes involved. In semiconductor systems, a full monolayer of surfactant is often used. For example, group V or VI elements have been used as surfactant in Si/Si(111) or Ge/Si(111) growth.[6] The use of a monolayer of surfactant passivates the substrate and enhances the adatom diffusion on the surfactant layer. Because of the weak bonding between the deposited adatom and the surfactant layer, the exchange of an adatom with a surfactant atom is exothermic and will therefore easily take place.[27–30] These changes will affect the 2D island pattern formation at submonolayer coverage in surfactant-mediated epitaxial growth. The 2D island pattern formation in surfactant-mediated epitaxial growth has only been studied experimentally very recently. In particular, the effect of a Pb monolayer as the surfactant in Ge growth on a Si(111) substrate has been studied systematically by Hwang *et al.*[31,32] and Chang *et al.*[33] They discovered a nucleation and growth behavior, which is in clear contradiction with traditional observations and expectations: they observed that large fractal islands were formed at low flux or high temperature, while small compact islands were formed at high flux or low temperature. Michely *et al.*[34] also observed a compact-to-fractal transition of Pt islands on Pt(111) when decreasing the deposition flux, this transition being possibly caused by the presence of the CO impurities.[35,36] In other experiments of Sb-induced growth of C_{60} films on NaCl(100),[37] a compact-fractal-compact transition was observed by increasing the temperature. The mechanism of such transitions is not yet clear.

In a recent paper,[38] we proposed a simple model to explain this transition which includes only three basic energy barriers: one against the diffusion of mobile adatoms on the surfactant terrace, one against the place exchange of mobile adatoms with their underneath surfactant atoms (seeding), and one against the aided place exchange of stuck adatoms with their underneath surfactant atoms. In the frame of this simple model, our kinetic Monte Carlo (KMC) simulations on a square lattice showed that fractal islands are formed at low deposition flux or high temperature and a transition to compact islands takes place when increasing the flux or decreasing the temperature. This is completely contrary to the prediction of classic DLA theory,[23–25] but is in excellent qualitative agreement with the experimental observations of Refs. 31 and 33. We also predicted that the temperature dependence of the island density exhibits a minimum at the temperature where the island shape transition takes place. We showed that the flux dependence of the island density can be separated into three different regimes: a weakly dependent regime, a scaling regime, and a saturated regime. We further rationalized the main finding through the realization that the island shape transition and the island density evolution are controlled by the shielding effect of the stuck adatoms on mobile adatoms. This effect prevents other incoming adatoms from joining the stable islands through the same sites. Because the creation of a seed for nucleation of a stable island and the subsequent growth are both exchange (or equivalently, reaction) limited, the formation of the stable islands are in the reaction limited aggregation (RLA) regime.

In this paper we systematically extend our previous study to a triangular lattice in order to to compare our results directly with those of the experiments.[31–33] We also note that the present investigation of the effect of a different substrate geometry is interesting scientifically in its own right. We also take into account the binding energy between the adatoms in the islands formed on the surfactant layer. This binding energy only hinders the diffusion process on the surfactant layer. The fractal-to-compact shape transitions are also observed when the deposition flux increases or when the growth temperature decreases. We furthermore obtain the characteristic dependence of the island density as a function of temperature (T) and the deposition flux (F). The same results are obtained qualitatively when we vary the basic potential-energy parameters of the model. We further study the case when dimers are stable on the surfactant terrace due to the existence of a binding energy, and when only these dimers can exchange with the surfactant atoms to become island seeds. Our KMC simulations on the square lattice show that the same fractal-to-compact island shape transition takes place, even if the temperature and flux dependence of the island density differ from the case of the monomer seed exchange. We also carry out a rate-equation analysis of the model in both the fractal and the compact island limits for the case where the island seeds only consist of monomers. In the fractal island limit, we derive a zero flux exponent, a constant coverage exponent, and an ascending temperature dependence. In the compact island limit, no analytical solution can be derived, and the rate equations are solved numerically. Besides other results consistent with the KMC simulations, we obtain a maximum at low temperature in the temperature dependence of island density.

The outline of this paper is as follows. We describe in Sec. II the basic assumptions of the reaction (exchange) limited aggregation model. In Sec. III we show the KMC results concerning the island evolution with the temperature and the deposition flux. The rate-equation analysis is then presented in Sec. IV. The results obtained are discussed and compared with experimental ones in Sec. V. Finally, a summary is given in Sec. VI.

II. THE REACTION (EXCHANGE) LIMITED AGGREGATION MODEL

As in Ref. 38, we start with an ideally flat substrate A and a complete monolayer of surfactant atoms S on the substrate. Adatoms B are randomly deposited on the surfactant terrace. The case $A \neq B$ corresponds to heteroepitaxial growth, while

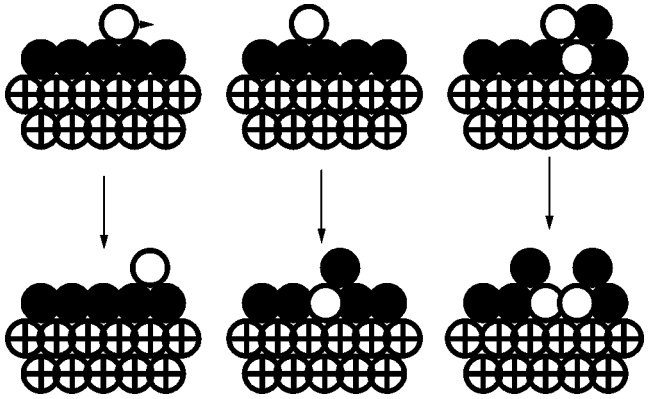

FIG. 1. Demonstration of the three elementary processes in the case of the monomer seed exchange: (a) diffusion of a free adatom on the surfactant terrace; (b) exchange of an adatom with the surfactant atom beneath it; (c) exchange of a stuck adatom with the surfactant atom beneath it, aided by the nearest dead atoms.

that at $A=B$ corresponds to homoepitaxial growth. We define three kinds of B atoms: the mobile active adatoms, the stuck active adatoms, and the dead adatoms. The active atoms are those remaining on the surfactant terrace, while the dead atoms are those that have exchanged positions with their underneath surfactant atoms. A stable island consists of dead atoms. Movable active adatoms may (a) diffuse on the surfactant terrace, (b) exchange positions with the surfactant atoms beneath them by overcoming a large energy barrier and become island seeds (seed exchange), or (c) stick to stable islands. A stuck adatom is still active. It must overcome another sizable barrier to exchange positions with the surfactant atom beneath it and become a member of the island (aided exchange). We make use of the name *aided exchange* because this exchange is assisted by the dead atoms of the island to which the stuck adatoms are sticking. We denote the diffusion barrier, the seed exchange barrier, and the aided exchange barrier by V_d, V_{se}, and $V_{ae}(<V_{se})$, respectively.

In Ref. 38, we limited the seed exchange to active monomers and our KMC simulations to growth on substrates with square geometry. In this paper we first extend our KMC simulations to growth on substrates with triangular geometry. We then extend to the case where addimers are the seed entities via collective place exchange with two surfactant atoms. The scientific motivation for considering addimer exchange is twofold. First, in many semiconductor systems a dimer is an elemental building block and can migrate collectively.[39] The other motivation is to check how the consideration of dimer exchange will change the scaling exponents in the temperature and flux dependence of the island density, as suggested in the experimental studies.[31–33]

A. The monomer seed exchange

We start with an ideally flat triangular lattice of material A covered with a complete layer of surfactant S. Atoms of material B are deposited onto the surfactant layer at a given deposition rate. A mobile adatom may (1) diffuse on the surfactant terrace [Fig. 1(a)], (2) hit and stick to an island of dead atoms, or (3) die directly by exchanging positions with the surfactant atom beneath it and form an island seed [Fig. 1(b)]. An adatom stuck to a stable island of dead atoms remains active for quite a long time, but it finally exchanges positions with the surfactant atom beneath it with a larger rate than the seed exchange rate [Fig. 1(c)]. An energy barrier V_d must be overcome for an adatom to hop successfully from one site of the lattice to a neighboring site. A large energy barrier V_{se} must be overcome for the exchange of an isolated adatom with the surfactant atom beneath it. Dead nearest-neighbor atoms help the place exchange of the stuck adatoms and the surfactant atoms, and the energy barrier against this exchange process is V_{ae}. The stuck adatoms act as shields and prevent other mobile adatoms from sticking to the dead atoms at the same sites. Islands formed on the surfactant terrace can still dissociate. According to the definition of classical nucleation theory, there are two critical island sizes: $i^*=\infty$ and $i^*=0$ for the upper layer of active adatoms and the lower layer of dead atoms, respectively. Over all, our model is consistent with the fact that the binding energy between A and B is typically much larger than the binding energy between A and S or B and S. The effect of the binding energy V_b between the adatoms is also investigated.

The elementary rates of the three processes: diffusion, seed exchange, and aided exchange, are defined by $R_d=\nu\exp(-V_d/kT)$, $R_{se}=\nu\exp(-V_{se}/kT)$, and $R_{ae}=\nu\exp(-V_{ae}/kT)$, respectively. The constant ν is the attempt frequency, and we neglect the possibility of having different attempt frequencies for the different processes. The hopping rate of a mobile adatom from a site i to its neighboring site already occupied by another adatom is zero. The bonding of an adatom at site i with adatoms in its nearest neighboring sites hinders its hopping. The hopping rate is therefore reduced to $R_d\exp(-n_bV_b/kT)$ if the adatom has n_b active adatoms as its nearest neighbors.

The four barriers satisfy the inequality chain $V_b\ll V_d<V_{ae}<V_{se}$. V_b has to satisfy the condition that even for a mobile adatom with the maximum number of neighbors (three on a square lattice and five on a triangular lattice), the barrier for an adatom to detach from an island on the surfactant layer is still much lower than the exchange barriers. V_d is the smallest among the remaining three barriers because adatom diffusion is often significantly enhanced due to the passivation of the substrate by the surfactant layer. V_{se} is the largest, making the formation of a nucleation center the rate-limiting process. A consequence of the second inequality ($V_d<V_{ae}$) is the existence of an effective repulsive wall surrounding the seed atom or an island of dead atoms. The existence of such a repulsive potential to the incoming adatoms due to the presence of the surfactant atoms surrounding an island has been proposed previously, and its effect on the island density has been explored very recently.[12,13] Here for simplicity, the in-plane mobility of the B atoms underneath the surfactant layer is considered to be negligible. We also ignore the reversal exchange process in which a B-type atom resurfaces to the top of the surfactant layer, which means that we consider the case where a B atom strongly favors the underneath site. When a B atom hops to a site which has n_d dead B-type nearest neighbors, it remains stuck there until it exchanges down with the rate n_dR_{ae}. This rate is used to emphasize the effect of B-type neighbors on the exchange process without introducing additional parameters.

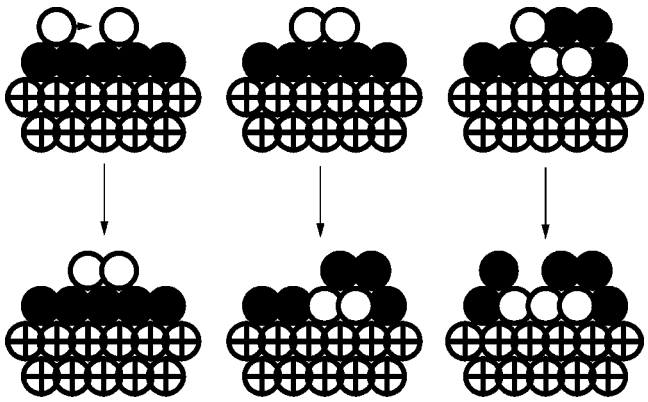

FIG. 2. Demonstration of the microscopic processes in the case of the dimer seed exchange. (a) Encounter of two active free adatoms on the surfactant terrace and formation of a dimer without overcoming any additional energy barrier. (b) Exchange of a dimer with the two surfactant atoms beneath it. (c) Exchange of a stuck single adatom with the surfactant atom beneath it, aided by the nearest dead dimer or island.

B. The dimer seed exchange

Recent studies of submonolayer growth on semiconductor[40] and metal surfaces[41,42] have suggested that, at low temperatures, the adatom density on the surface is so high that the stable nucleus is no longer an isolated atom, but rather a dimer. It has also been reported that these dimers can exchange positions with the surfactant atoms underneath and become a nucleation center in the surfactant-mediated growth.[43] Because the weak bonds between *A* and *S* atoms and between *B* and *S* ones are replaced by the strong bonds between *A* and *B* without breaking the strong *B*-*B* bonds, the collective exchange of the *B*-type dimers is energetically favorable. To examine the effect of such collective motion, we carry out KMC simulations with dimers as stable nuclei. When two adatoms meet on the surfactant terrace, they form a dimer without needing to overcome any barrier [Fig. 2(a)]. The dimer formed is stable, since the energy barrier against dissociation is high. Once this dimer exchanges with surfactant atoms, it dies and becomes an island seed [Fig. 2(b)]. Subsequently arriving single adatoms stick to the seed, and finally exchange with the surfactant atoms beneath them, becoming a part of the stable island [Fig. 2(c)]. The relative ordering between the diffusion barrier V_d, the seed exchange barrier V_{se}, and the aided exchange barrier V_{ae} is the same as in the case of monomer exchange. The only difference is that the *B*-*B* binding energy within a dimer is considered to be much higher than the binding energy between adatoms in an island formed on the surfactant terrace.

III. KMC SIMULATIONS

A. The case of the monomer seed exchange

KMC simulations are carried out on a 200×200 triangular lattice. The simulation parameters are as follows. A small diffusion barrier $V_d=0.59$ eV is chosen, reflecting that adatoms quickly diffuse on the surfactant terrace. The barriers of the seed exchange and the aided exchange processes are set equal to $V_{se}=0.90$ eV and $V_{ae}=0.82$ eV, respectively. Another set of barriers $(V_d,V_{se},V_{ae})=(0.53,0.88,0.79$ eV) is also used for comparison. We vary the growth temperature from 285 to 425 K, and the deposition flux from 0.0001 to 0.04 ML/s. No binding energy between the B adatoms is considered in this first part. The temperature dependence of the island shape obtained with $F=0.005$ ML/s and $\theta=0.1$ ML is shown in Fig. 3. It can be seen on Fig. 3(a), which represents the island pattern at 425 K, that the islands are typically fractal-like. When the temperature is decreased to 320 K, and then to 310 K, the islands become more compact, as shown on Figs. 3(b) and 3(c), respectively. Figure 3(d) is obtained at 285 K, and the islands are completely compact. This evolution is in good agreement with the results of the experiments of Refs. 31–33. A transition temperature between fractal and compact islands can be defined, and is situated in this case between 310 and 320 K. Figure 4 shows an interesting nonmonotonic dependence of the island density with the temperature. It can be seen that the minimum of the curve is located around the temperature for which the compact-to-fractal transition in island morphology has been observed. The descending part of the curve corresponds to compact islands, while the ascending part corresponds to fractal-like islands.

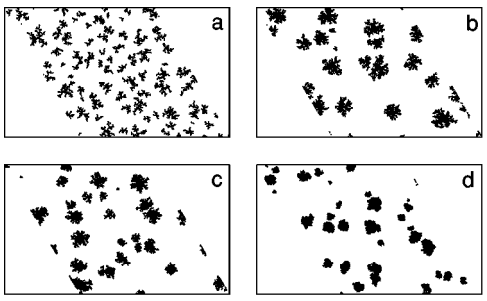

FIG. 3. Island shapes obtained on a triangular lattice in the monomer seed exchange case for a deposition flux equal to 0.005 ML/s, a 0.1 ML coverage, and with zero binding energy in the islands on the surfactant terrace, at different temperatures: (a) 425 K, (b) 320 K, (c) 310 K, and (d) 285 K.

We know in our case, the rate-limiting process for the nucleation of a stable island is the diving of an adatom into the sublayer; therefore, our system is always in the exchange

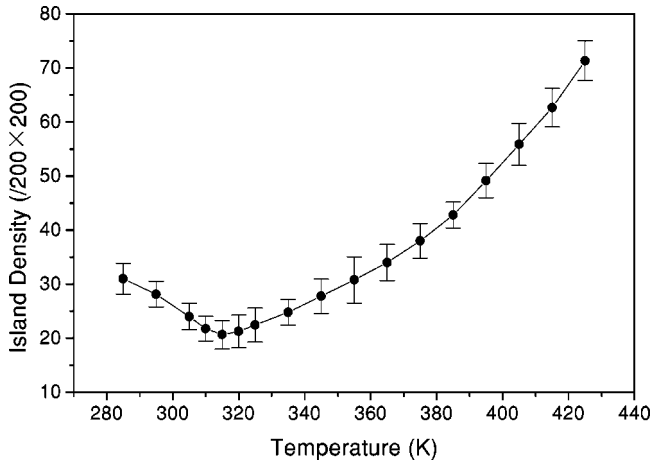

FIG. 4. Temperature dependence of the island density on a triangular lattice in the monomer seed exchange case at 0.005 ML/s deposition flux, 0.1 ML coverage, and with a zero binding energy.

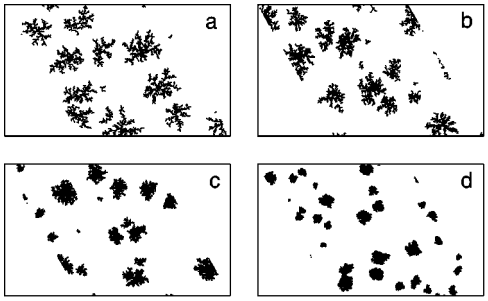

FIG. 5. Island shapes obtained on a triangular lattice in the monomer seed exchange case at 300 K, 0.1 ML coverage, and with a zero binding energy, for different deposition flux: (a) 0.0001 ML/s, (b) 0.0005 ML/s, (c) 0.0025 ML/s, and (d) 0.04 ML/s.

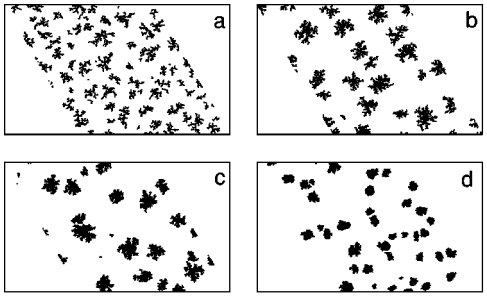

FIG. 7. Island shapes obtained on a triangular lattice in the monomer seed exchange case at 0.005 ML/s deposition flux and 0.1 ML coverage for different temperatures: (a) 425 K, (b) 320 K, (c) 310 K, and (d) 285 K. The binding energy V_b is set to 0.04 eV.

prominent region. When the temperature is low, a stable seed atom in the surfactant layer may not necessarily grow into a stable island because of the effective shielding of the incoming adatoms but those seeds which mange to grow into islands will grow even faster as their sizes increase. The decrease in island density with temperature is caused by the increased mobility of the adatoms in searching for such islands. On the other hand, after the transition temperature, the shielding effects are very weak, and every seed atom is likely to grow into a stable island. The island density increase with temperature reflects the enhanced rate in creating such seeds.

The flux dependence of the island shape obtained at 300 K and for a coverage $\theta=0.1$ ML is shown in Fig. 5. Figures 5(a)–5(d) represent the islands obtained with the flux equal to 0.0001, 0.0005, 0.0025, and 0.04 ML/s, respectively. The island shape transition from large fractal islands to small compact islands when the deposition flux increases can be clearly seen. This is again in good agreement with the results of the experiments of Refs. 31–33. Figure 6 shows the flux dependence of the stable island density, N_s, obtained at $T=300$ K and $\theta=0.1$ ML. It can be seen that the island density increases rapidly at small deposition flux, and becomes nearly saturated at large flux. To quantify the dependence, we plot in the insert the evolution of the density as a function of the logarithm of the flux. This curve can be divided into three regimes: the low-flux fractal regime, where the dependence is very weak; the intermediate-flux regime, where a scaling law, $N_s \sim F^{\beta}$ with $\beta=0.22$, can be defined; and the high-flux compact regime, where the island density has saturated.

We next add a binding energy between the B adatoms that have only one active nearest-neighbor adatom, and set this binding energy (V_b) to 0.04 eV. We then carry out KMC simulations as previously. Figures 7 and 8 show the new temperature dependence of the island shape and of the island density obtained with $F=0.005$ ML/s and $\theta=0.1$ ML. They are very similar to those obtained without the binding energy. The island shape transition from large fractal islands to small compact islands when the temperature decreases can be clearly seen. The difference is that the minimum of the island density as a function of the temperature is located at approximately 320 K. There is no detectable shift in the minimum temperature. Figures 9 and 10 show the new flux dependence of the island shape and of the island density at 300 K and for a 0.1 ML coverage. Again, these results are very similar to the previous ones: we can clearly see the island shape transition from large fractal islands to small compact islands when the deposition flux increases, and the island density exhibits the same three regimes as a function of the logarithm of the deposition flux. The scaling exponent

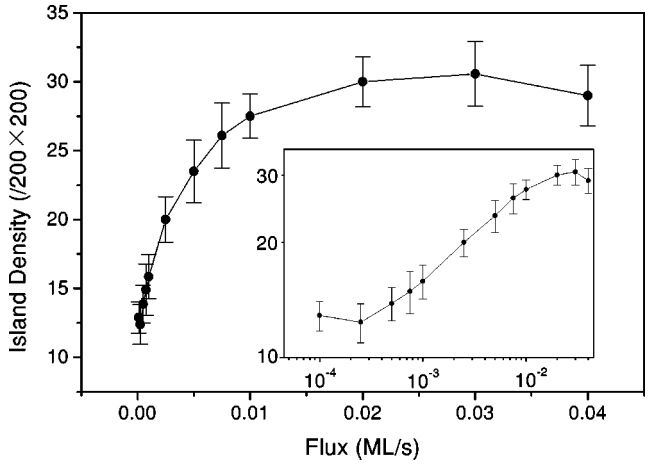

FIG. 6. Deposition flux dependence of the island density on a triangular lattice in the monomer seed exchange case at 300 K and a 0.1 ML coverage, with a zero binding energy in the islands on the surfactant terrace.

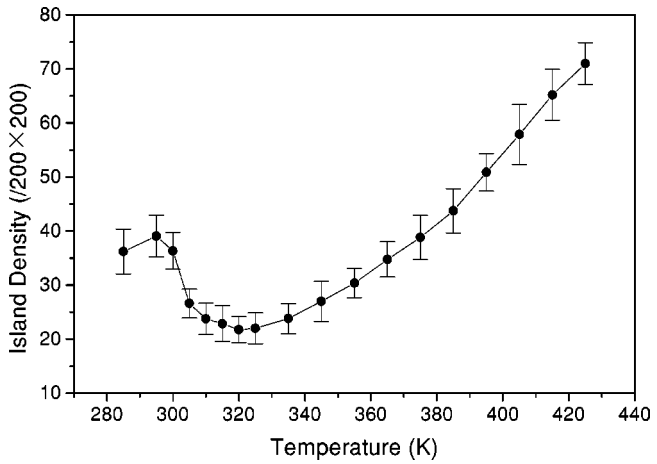

FIG. 8. Temperature dependence of the island density on a triangular lattice in the monomer seed exchange case at 0.005 ML/s deposition flux and 0.1 ML coverage. The binding energy V_b is set to 0.04 eV.

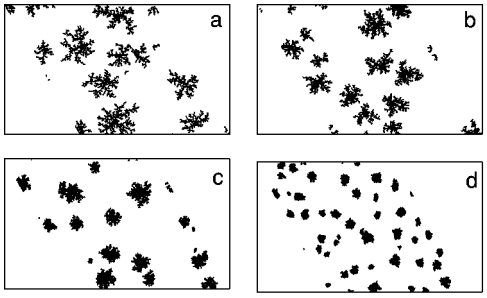

FIG. 9. Island shapes obtained on a triangular lattice in the monomer seed exchange case at 300 K and 0.1 ML coverage for different deposition flux: (a) 0.0001 ML/s, (b) 0.0005 ML/s, (c) 0.002 ML/s, and (d) 0.04 ML/s. The binding energy in the islands on the surfactant layer is set to 0.04 eV.

in the intermediate-flux regime is in this case equal to 0.40. It is larger than the previous scaling exponent 0.22 in the case of the zero binding energy. The binding energy hinders the mobility of the adatoms on the surfactant terrace. As a result, more seed exchanges take place and more new islands form on the surfactant terrace, leading to higher island density.

B. The case of the dimer seed exchange

In this case, the KMC simulations are carried out on a square lattice. We are interested here in the quantitative changes in the temperature and flux dependence of the island density. As in the previous paper[38] and in Sec. III A, the diffusion, seed exchange, and aided exchange barriers are set to $(V_d, V_{se}, V_{ae}) = (0.59, 0.90, 0.82$ eV), respectively. We vary the growth temperature from 285 to 425 K, and the deposition flux from 0.0001 to 0.04 ML/s. The B-B binding energy in a dimer is set equal to 0.13 eV, and the detachment energy of an adatom bonded to an island through one adatom is 0.02 eV.

Figure 11 shows the simulated island patterns and their flux evolution as a function of the deposition flux at 300 K and for a coverage of 0.1 ML. As in the monomer seed exchange case, a transition from large fractal islands to small compact islands is observed when the deposition flux increases. We have plotted in Fig. 12 the flux dependence of the island density at 300 K and for a 0.1 ML coverage. Again the curve as a function of the logarithm of the flux can be divided into three regimes, and the scaling exponent in the intermediate-flux regime is in this case equal to 0.48. This exponent is larger than the one we obtained in the monomer seed exchange case ($\beta = 0.40$),[38] but still much smaller than the exponent 1.76 found in experiments.[31]

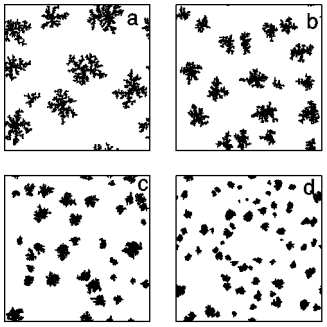

FIG. 11. Island shapes obtained on a 200×200 square lattice in the dimer seed exchange case at 300 K and 0.1 ML coverage for different deposition flux: (a) 0.0001 ML/s, (b) 0.0005 ML/s, (c) 0.0015 ML/s, and (d) 0.02 ML/s.

Figure 13 shows the simulated island patterns and their temperature evolution for a 0.005 ML/s deposition flux and 0.1 ML coverage. As previously, the islands formed change from fractal-like to compact when the temperature decreases. We represented on Fig. 14 the temperature dependence of the island density. It can be seen that the island density decreases monotonically when the temperature increases, and that there is no minimum at the compact-to-fractal transition temperature (315 K). Here the temperature dependence of the island density can be interpreted qualitatively as follows: at high temperatures, the kinetic energy of the thermal motion is large enough to break the B-B bonds within the dimers formed on the surfactant terrace, so that there are less active dimers on the surfactant terrace. The probability of formation of an island seed is therefore small. On the other hand, at low temperatures, the dimers are more stable, so that more active dimers exist on the surfactant terrace, and the probability of forming a nucleation seed is therefore larger.

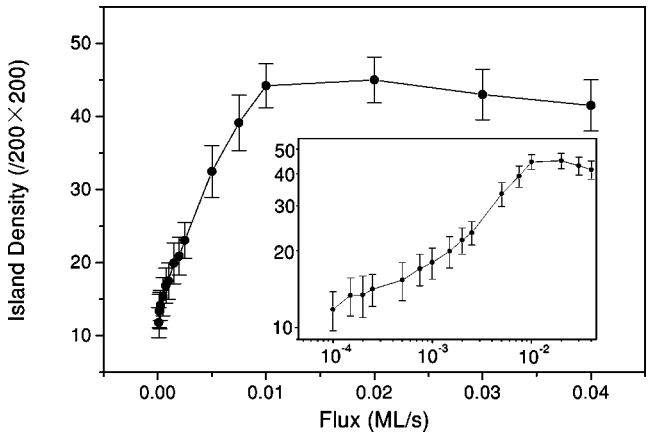

FIG. 10. Deposition flux dependence of the island density on a triangular lattice in the monomer seed exchange case at 300 K and 0.1 ML coverage of 0.1 ML. The binding energy V_b in the islands on the surfactant layer is set as 0.04 eV.

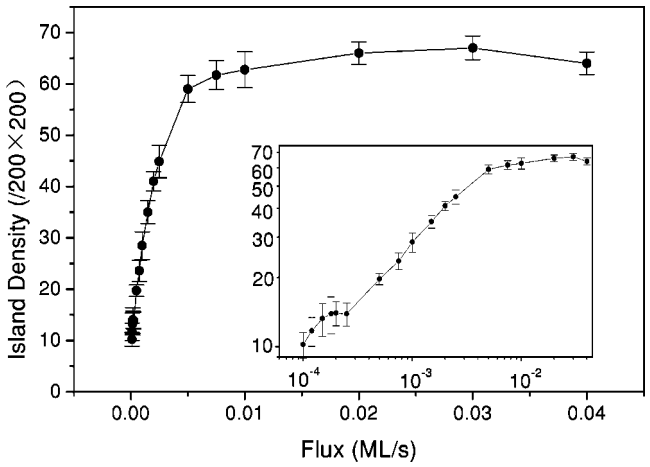

FIG. 12. Deposition flux dependence of the island density on a 200×200 square lattice in the dimer seed exchange case at 300 K and 0.1 ML coverage.

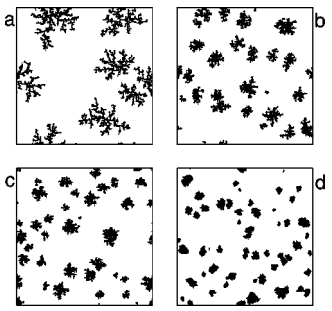

FIG. 13. Island shapes obtained on a 200×200 square lattice in the dimer seed exchange case at 0.005 ML/s deposition flux and 0.1 ML coverage for different temperatures: (a) 425 K, (b) 320 K, (c) 310 K, and (d) 285 K.

IV. RATE-EQUATION ANALYSIS

As shown above, KMC simulation can directly produce island shape and density. But, a large variation of model parameters is not possible because of limited computer power. Rate-equation analysis is a powerful tool in this aspect. We shall do a rate-equation analysis of the above model in the case of the monomer seed exchange. In this approach we introduce the island perimeter L_d and calculate the area of an island as $S_d=pL_d^q$, where p is a constant and q is the dimensionality of the island.[24,25] For compact islands, q is equal to 2, while for fractal islands q is the fractal dimension, and is therefore between 1 and 2. In the low-coverage limit, we consider the following rate equations:

$$\frac{d}{dt}n_a=F\theta(t_0-t)-\alpha_d n_a-c\alpha_b n_a(N_sL_d-gn_b), \quad (1)$$

$$\frac{d}{dt}n_b=-\alpha_e n_b+c\alpha_b n_a(N_sL_d-gn_b), \quad (2)$$

$$\frac{d}{dt}N_s=\alpha_d n_a, \quad (3)$$

where n_a is the density of the mobile active atoms, n_b is the density of the stuck active atoms, α_b, α_d, and α_e are coefficients which in first approximation can be chosen as the rates R_d, R_{se}, and R_{ae}, respectively, c is the capture constant, and g the geometry factor. We have introduced the step function $\theta(t_0-t)$, where t_0 is the time at which the deposition is ended, to take into account the fact that the STM imaging is typically done a few hours after the end of the deposition.[31,33] The parameters p, q, c, and g are dependent on the lattice geometry.

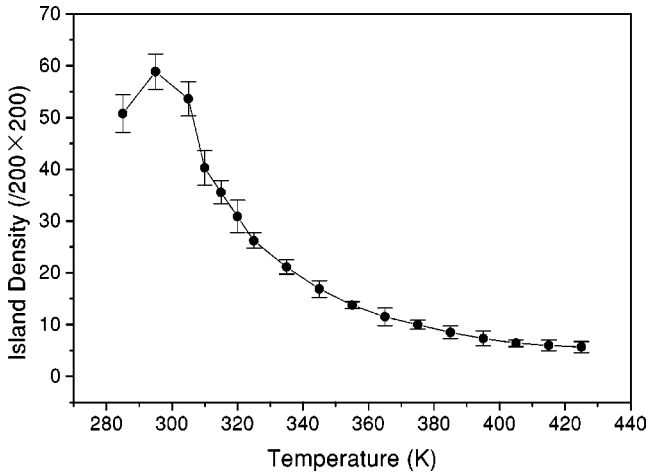

FIG. 14. Temperature dependence of the island density on a 200×200 square lattice in the dimer seed exchange case at 0.005 ML/s deposition flux and 0.1 ML coverage.

In Eq. (1), the term containing F describes the adatom deposition, the second term reflects the exchange of positions between a mobile adatom and the surfactant atom beneath it and the creation of a seed, and the last term describes the capture of a mobile adatom by a stable island. This atom is then stuck to the island, but is still active so that it cannot capture other mobile adatoms. In Eq. (2), the α_e term describes the exchange of stuck but still active adatoms with surfactant atoms.

Let N_a be the total density of active atoms: $N_a=n_a+n_b$. The density of dead atoms N_d can be expressed in term of N_a: $N_d=Ft_s-N_a$, where t_s is the smaller of t and t_0. Because the average island size S_d is defined by $S_d=N_d/N_s$, the perimeter L_d can be expressed as follows:

$$L_d=\left(\frac{Ft_s-n_a-n_b}{pN_s}\right)^{1/q}. \quad (4)$$

The mobile adatom density n_a, the total active adatom density N_a, and the stable island density N_s can be obtained from Eqs. (1) to (4).

At low flux or high temperature, i.e., in the fractal regime, very few adatoms remain active at the end of the deposition. The island shape is then mainly determined by the $t<t_0$ region. After a certain deposition time, the island growth is in the steady growth regime, and a steady-state approximation can be used for N_a, as done in previous studies.[12,13,8,15,24,25] In those studies, the active adatom density was taken to be a constant after the growth entered the regime of steady growth. But, for the surfactant-mediated growth, the constant term, the leading term, is not accurate enough to describe the active adatom density; a further term is necessary for a more realistic description of it in the case of the surfactant-mediated growth. Therefore, we choose to use the quasi-steady-state approximation, where the evolution of N_a is described as follows:

$$N_a=c_1+c_2t^{-m}, \quad (5)$$

where c_1, c_2, and m are constants to be determined. Substituting N_a into Eqs. (1) to (4), we obtain $c_1=F/\alpha_e$ and the asymptotic behavior of the stable island density N_s:

$$N_s=c_3\theta^{(q-1)/(2q-1)}\left[\exp\left(-\frac{V_{se}-V_d}{kT}\right)\right]^{q/(2q-1)}, \quad (6)$$

where c_3 is a constant independent of temperature, coverage, or flux. A scaling law of the island density can then be derived: $N_s\sim\{\exp[-(V_{se}-V_d)/kT]\}^{n_T}F^{n_F}\theta^{n_\theta}$, where $n_T=q/(2q-1)$, $n_F=0$, and $n_\theta=(q-1)/(2q-1)$. The zero flux exponent n_F is consistent with the results of our KMC simulations. The constant q can only be easily determined from the island shape in the limit of very low flux or very high tem-

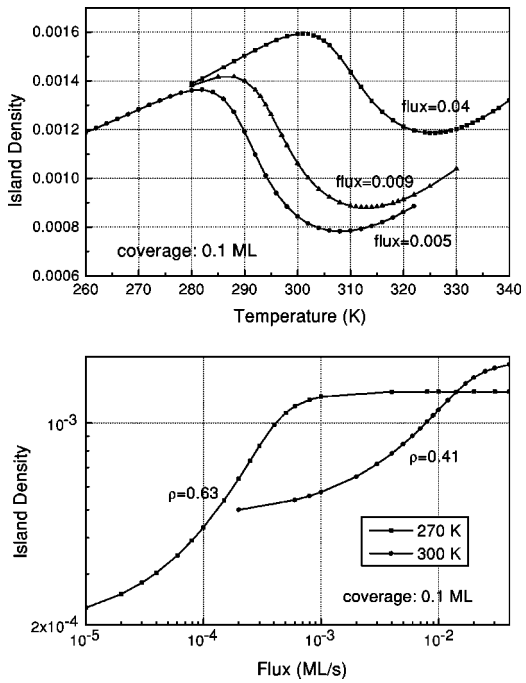

FIG. 15. Numeric solutions of the rate equations in the compact island limit. The upper part shows the temperature dependence of the island density at 0.1 ML coverage for three flux values: 0.005 ML/s, 0.009 ML/s, and 0.04 ML/s. The lower part shows the flux dependence of the island density at 300 and 270 K and 0.1 ML coverage. At 300 K, a scaling law with an exponent 0.41 can be defined in the intermediate flux region. At 270 K, the saturation of the island density in the high flux region is very clear and a scaling law with an exponent 0.63 can be defined.

perature, because in this case we are in the ideal fractal regime. The geometry factor g is irrelevant in this regime.

In the compact and intermediate regimes, both the $t<t_0$ and $t>t_0$ regions must be considered. The growth is never in a steady growth state, making it impossible to obtain an analytical solution of the rate equations. We therefore look for numeric solutions, and replace the derivative of a function $y(t)$ by the finite differential as follows:

$$\frac{dy(t)}{dt}=\frac{y(t+\Delta t)-y(t)}{\Delta t}, \tag{7}$$

where Δt is the time increment. Since we are considering compact islands, we take $q=2$. p is then equal to 1 for a square island, and to $\pi/4$ for a circular island. We choose $p=0.8$ since our islands are more similar to circles. Then only two parameters (c and g) need to be determined, and we obtain them through comparison with the KMC simulations. We choose $c=0.5$ and $g=0.2$ to reproduce approximately the saturated island density and the scaling exponent of the island density flux dependence at 300 K and 0.1 ML coverage.

The upper part of Fig. 15 shows the temperature dependence of the compact island density at 0.1 ML coverage for flux equal to 0.005, 0.009, and 0.04 ML/s. For flux equal to 0.005 ML/s, the island density exhibits a minimum at $T_n=310$ K, as well as a maximum at $T_x=280$ K. This latter temperature was not accessed in the KMC simulation on the square lattice[38] although it seems to appear in the KMC simulation on the triangular lattice (Fig. 8). This maximum means that the island density decreases with the temperatures decreasing in the very-low-temperature region. This may be explained by the fact that at very low temperature the ratio R_{se}/R_{ae} decreases exponentially with the temperature decreasing, and that an adatom prefers sticking to an existing island and then exchanging with a surfactant atom with the rate R_{ae}, rather than exchanging directly with the rate R_{se}. With temperature decreasing, the island density first decreases due to the decreasing seed exchange; then increases because the increasing shielding effect makes more new islands appear; and then decreases because the ratio R_{se}/R_{ae} decreases rapidly. The low-temperature region $T<T_x$ and high-temperature region $T>T_n$ both are dominated by the seed exchange. The intermediate temperature region $T_x<T<T_n$ is dominated by the shielding effect. Both T_x and T_n are increasing with flux because the shielding effect increases with the flux. The difference between the minimal and maximal island densities decreases with flux increasing. This may result from the same flux dependence of the two transition temperatures T_x and T_n.

The lower part of Fig. 15 shows the flux dependence of the compact island density at 300 and 270 K for a coverage of 0.1 ML. In the high flux region the island density becomes saturated when the flux increases. In the intermediate flux region, a scaling law can be defined, and the scaling exponent is 0.41 and 0.63 for 300 and 270 K, respectively. The exponent at 300 K is almost equal to the one obtained in the KMC simulation. In the low flux region the island density depends less on the flux, which is consistent with the zero flux exponent obtained in the fractal limit. The coverage dependence of the compact island density is divided into three well-defined scaling regimes, with the scaling exponents n_1, n_2, and n_3 for the low, intermediate, and high coverage domains, respectively. At 300 K and for a flux of 0.005 ML/s, n_1 is equal to 0.49, n_2 to 0.57, and n_3 to 0.21. When the flux increases, the n_1 and n_2 exponents increase, while the high coverage exponent n_3 decreases.

Summarizing this section, we have carried out rate-equation analysis of the RLA model in both the fractal and the compact regimes. In the fractal regime, we have obtained constant scaling exponents independent of the growth parameters. In the compact regime scaling laws can be defined as well, but the scaling exponents depend on the temperature, the flux, the barrier energies, etc. In this regime, the post deposition time ($t>t_0$) plays an essential role in the growth, and has a big effect on the resultant island density. This is completely different from the steady-state growth in the fractal regime. For the islands in the intermediate region, q can at first approximation be set to 2, and the numerical solutions obtained in the compact island regime can be extended to the intermediate regime.

V. DISCUSSION AND CONCLUSION

The KMC simulations described in our previous letter[38] and the extended KMC simulations and rate-equation analysis presented in this paper show that in various cases of surfactant-mediated growth fractal islands are obtained at high temperature or low flux, and that compact islands are formed at low temperature or high flux. These results are in

contradiction with the hit-stick-relax scenario of the classic DLA theory,[23,24] where one expects fractal islands at low temperature or high flux and compact islands in the opposite limits. The difference comes from the fact that the limiting process in the formation of stable islands is diffusion in DLA, while it is the exchange of adatoms with surfactant atoms in our RLA model. In DLA theory, the island seeds have a kinetic origin and stuck adatoms join the stable islands at once or within a very short relaxing time after they hit the islands. In our case, the island seeds result from the exchange of adatoms with surfactant atoms and a stuck adatom can remain active and not as part of a stable island for a very long time after hitting the island. Because this adatom is still active and is surrounded by the surfactant atoms, other incoming adatoms cannot stick to it. Therefore, the effective island edges, where adatoms can stick, are reduced. Stuck adatoms thus act as shields in preventing other incoming adatoms from sticking to stable islands through their sites. This shielding effect[38] is determined by the ratio of a stuck adatom lifetime to the time interval between two successive hits of incoming adatoms. At very high temperature the stuck adatom lifetime is very short, and at very low flux, the interval between two successive hits becomes very long. In these two cases, the shielding effect is very weak, so that we obtain ideal fractal islands. On the other hand, at low temperature or high flux, the islands are almost completely surrounded by stuck but still active adatoms, so that the shielding effect is very strong. The probability for incoming adatoms to successfully stick to an island becomes very small. Adatoms have to come and go many times before finding a free edge site to stick to. This is effectively equivalent to the relaxation after the hit-and-stick scenario in DLA theory, and the islands formed are therefore compact.

It can be seen from our simulations that the shielding effect does not change qualitatively when additional factors, such as binding energy between active adatoms on the surfactant terrace, different lattice geometry, or possible simultaneous exchange of several adatoms (dimer), are considered. In both the monomer and dimer seed exchange cases, the flux dependence of the island density can be divided into three regions. In the low flux region, the flux dependence is very weak, while in the intermediate region, a scaling law, $N_s \sim F^{\beta}$, can be defined. On a square lattice, β is equal to 0.40 in the case of the monomer seed exchange[38] and to 0.48 in the case of the dimer seed exchange. The scaling exponent therefore increases when the possibility of simultaneous exchange of several adatoms is included. Furthermore, on the triangular lattice, β is equal to 0.22 if there is no energy barrier to the detachment of an adatom from an island formed on the surfactant terrace, and is greater than 0.22 if such a barrier is considered. The scaling exponent therefore increases with the binding energy. These trends might enable us to reproduce the larger scaling exponent found in the experiments.[31,32] As for the temperature dependence of the island density, the compact-to-fractal transition happens at approximately the same temperature, about 320 K, in all cases. In the monomer seed exchange case, the island density curve exhibits a minimum at this transition temperature. In the case of the dimer seed exchange, on the other hand, the island density is a nearly monotonically decreasing function of the temperature, without a minimum at the compact-to-fractal transition temperature. This is due to the fact that the dimers are more stable at low temperature, so that the probability of nucleation is larger, which results in the formation of a higher number of islands. If we compare the results of our simulation to the experiments of heteroepitaxial growth, where $A = \mathrm{Si}$, $S = \mathrm{Pb}$, and $B = \mathrm{Ge}$, [31,33] it can be seen that our model reproduces the main qualitative findings of the experiment, namely, the islands formed are small and compact at high deposition flux or low temperature, and are large and fractal at low deposition flux or high temperature. For a more realistic model of surfactant-mediated growth, other elementary processes would have to be considered, such as the relaxation of incoming adatoms hitting an island to a site of lower energy, or the motion, with a small but finite probability, of adatoms beneath the surfactant layer. The introduction of these processes would allow us to reproduce the experimental results more accurately. Furthermore, our model and results are also applicable to surfactant-mediated homoepitaxial growth.[34] Finally, the fractal-to-compact transitions described here are expected to be observed even if the stable islands are formed on the substrate, but are surrounded by a sufficiently high coverage of impurity atoms, as long as those impurities effectively hinder the growth of the stable islands by preventing the incoming adatoms from joining them.

VI. SUMMARY

We have extended the range of applicability of the RLA model presented in our previous letter to various more realistic growth systems: We have carried out KMC simulations on a triangular lattice and varied the four main parameters of the model. We have also considered additional physical processes, such as the detachment of an adatom trapped by an island formed on the surfactant layer, or the possibility of simultaneous exchange of two adatoms (dimer) with surfactant atoms. These lattice and parameter variations, as well as the generalizations beyond the previous model, do not change the key findings of the model: Fractal-to-compact transition can be induced either by decreasing the growth temperature or by increasing the deposition flux. Of course, on a quantitative level, the evolution of the island density differs depending on the phenomena considered and the parameters chosen. There are a maximum and a minimum in the temperature dependence of the island density in the monomer seed exchange case. On the other hand, in the case of the dimer seed exchange, the island density is a monotonously decreasing function of the temperature in the high-temperature domain. Furthermore, in all cases, the flux dependence of the island density can be divided into three different regions: a weak dependence region at low flux, a scaling region at intermediate flux, and a saturation region at high flux. The scaling exponent in the intermediate region is larger in the dimer seed exchange case than in the monomer seed exchange case, but still smaller than the exponent found in experiments.[31] Because the stable islands consist of the dead atoms that have exchanged positions with the surfactant atoms beneath them, the nucleation and the growth of the islands are both exchange limited. In this case, the physical process controlling the island shape transition is the shielding effect of adatoms stuck to stable islands on incoming adatoms.

ACKNOWLEDGMENTS

We are deeply obligated to Dr. Marjorie Bertolus for her critical reading of the manuscript, and her numerous helpful suggestions. This research was supported by the Natural Science Foundation of China (Grant Nos. 19 810 760 328 and 19 928 409), by the Chinese Department of Science and Technology under the State Key Project of Basic Research (Grant No. G1999064509), by Oak Ridge National Laboratory, managed by Lockheed Martin Energy Research Corp. for the U.S. Department of Energy under Contract No. DEAC05-96OR22464, and by the U.S. National Science Foundation (Grant No. DMR-9705406).

[1] M. Copel, M. C. Reuter, E. Kaxiras, and R. M. Tromp, Phys. Rev. Lett. **63**, 632 (1989).

[2] H. A. van der Vegt, H. M. van Pinxteren, M. Lohmeier, E. Vlieg, and J. M. C. Thornton, Phys. Rev. Lett. **68**, 3335 (1992).

[3] J. Camarero, L. Spendeler, G. Schmidt, K. Heinz, J. J. de Miguel, and R. Miranda, Phys. Rev. Lett. **73**, 2448 (1994); J. Camarero, T. Graf, J. J. de Miguel, R. Miranda, W. Kuch, M. Zharnikov, A. Dittschar, C. M. Schnieder, and J. Kirschner, *ibid.* **76**, 4428 (1996); J. J. de Miguel (private communication).

[4] W. Wulfhekel, N. N. Lipkin, J. Kliewer, G. Rosenfeld, L. C. Jorritsma, B. Poelsema, and G. Gomsa, Surf. Sci. **348**, 227 (1996); A. M. Begley, S. K. Kim, J. Quinn, F. Jona, H. Over, and P. M. Marcus, Phys. Rev. B **48**, 1779 (1993); N. Memmel and E. Bertel, Phys. Rev. Lett. **75**, 485 (1995); H. Wolter, M. Schmidt, and K. Wandelt, Surf. Sci. **298**, 173 (1993); V. Scheuch, K. Potthast, Bert Voigtländer, and H. P. Bonzel, *ibid.* **318**, 115 (1994).

[5] D. J. Eaglesham and M. Cerullo, Appl. Phys. Lett. **58**, 2276 (1991); M. Copel and R. M. Trom, *ibid.* **58**, 2648 (1991).

[6] Bert Voigtländer, Andre Zinner, Thomas Weber, and Hans P. Bonzel, Phys. Rev. B **51**, 7583 (1995).

[7] M. Copel and R. M. Tromp, Phys. Rev. Lett. **72**, 1236 (1994); H. Wado, T. Schimizu, M. Ishida, and T. Nakamura, J. Cryst. Growth **147**, 320 (1995); J. Massies and N. Grandjean, Phys. Rev. B **48**, 8502 (1993); E. Tournie, N. Grandjean, A. Trampert, J. Massies, and K. H. Ploog, J. Cryst. Growth **150**, 460 (1995); G. Mendoza-Diaz, S. Stevens, A. F. Schwartzman, and R. Beresford, *ibid.* **178**, 45 (1997).

[8] See, for example, W. F. Egelhoff, Jr., P. J. Chen, C. J. Powell, M. D. Stiles, and R. D. McMichael, J. Appl. Phys. **79**, 2491 (1996), and references therein. See also Z. Y. Zhang and M. G. Lagally, Science **276**, 377 (1997); D. Kandel and E. Kaxiras, cond-mat/9901177 (unpublished).

[9] J. Vrijmoeth, H. A. van der Vegt, J. A. Meyer, E. Vlieg, and R. J. Behm, Phys. Rev. Lett. **72**, 3843 (1994).

[10] E. Kaxiras, Europhys. Lett. **21**, 685 (1993); Thin Solid Films **272**, 386 (1996).

[11] V. Fiorentini, S. Oppo, and M. Scheffler, Appl. Phys. A: Mater. Sci. Process. **60**, 399 (1995); J. Neugebauer, T. Zywietz, M. Scheffler, J. E. Northrup, and Ch. G. Van de Walle, Phys. Rev. Lett. **80**, 3097 (1998).

[12] I. Markov, Phys. Rev. B **50**, 11 271 (1994).

[13] D. Kandel, Phys. Rev. Lett. **78**, 499 (1997).

[14] Z. Zhang and M. G. Lagally, Phys. Rev. Lett. **72**, 693 (1994).

[15] D. Kandel and E. Kaxiras, Phys. Rev. Lett. **75**, 2742 (1995).

[16] D. J. Eaglesham, F. C. Unterwald, and D. C. Jacobson, Phys. Rev. Lett. **70**, 966 (1993); R. Kern and P. Müller, J. Cryst. Growth **146**, 193 (1995).

[17] R. Q. Hwang, J. Schröder, C. Günther, and R. J. Behm, Phys. Rev. Lett. **67**, 3279 (1991).

[18] T. Michely, M. Hohage, M. Bott, and G. Comsa, Phys. Rev. Lett. **70**, 3943 (1993).

[19] H. Röder, E. Hahn, H. Brune, J. P. Bucher, and K. Kern, Nature (London) **366**, 141 (1993); H. Brune, C. Romainczyk, H. Röder, and K. Kern, *ibid.* **369**, 469 (1994); H. Röder, K. Bromann, H. Brune, and K. Kern, Phys. Rev. Lett. **74**, 3217 (1995); H. Brune, Surf. Sci. Rep. **31**, 121 (1998).

[20] P. Meakin, Phys. Rev. A **27**, 1495 (1983).

[21] J. Jacobsen, K. W. Jacobsen, and J. L. Nørskov, Surf. Sci. **359**, 37 (1996).

[22] T.-Y. Fu, Y.-R. Tzeng, and T.-T. Tsong, Phys. Rev. B **54**, 5932 (1996).

[23] T. A. Witten and L. M. Sander, Phys. Rev. Lett. **47**, 1400 (1981).

[24] Z. Y. Zhang, X. Chen, and M. G. Lagally, Phys. Rev. Lett. **73**, 1829 (1994).

[25] J. W. Evans and M. C. Bartelt, J. Vac. Sci. Technol. A **12**, 1800 (1994); J. G. Amar and F. Family, Phys. Rev. Lett. **74**, 2066 (1995); G. S. Bales and D. C. Chrzan, *ibid.* **74**, 4879 (1995).

[26] Shudun Liu, Lutw Bonig, John Detch, and Horia Metiu, Phys. Rev. Lett. **74**, 4495 (1995); Shudun Liu, Zhenyu Zhang, George Comsa, and Horia Metiu, *ibid.* **71**, 2967 (1993).

[27] R. M. Tromp and M. C. Reuter, Phys. Rev. Lett. **68**, 954 (1992).

[28] B. D. Yu and A. Oshiyama, Phys. Rev. Lett. **72**, 3190 (1994); B. D. Yu, T. Ide, and A. Oshiyama, Phys. Rev. B **50**, 14 631 (1994).

[29] Y.-J. Ko, J.-Y. Yi, S.-J. Park, E.-H. Lee, and K. J. Chang, Phys. Rev. Lett. **76**, 3160 (1996).

[30] K. Schroeder, B. Engels, P. Richard, and S. Blugel, Phys. Rev. Lett. **80**, 2873 (1998).

[31] I.-S. Hwang, T.-C. Chang, and T. T. Tsong, Phys. Rev. Lett. **80**, 4229 (1998).

[32] Ing-Shouh Hwang, Tien-Chih Chang, and Tien T. Tsong, Surf. Sci. **410**, L741 (1998).

[33] T.-C. Chang, I.-S. Hwang, and T. T. Tsong, Phys. Rev. Lett. **83**, 1191 (1999).

[34] T. Michely, M. Hohage, and G. Comsa, in *Surface Diffusion: Atomistic and Collective Processes*, edited by M. C. Tringides and M. Scheffler, NATO Advanced Studies Institute, Series B: Physics, Vol. 360 (Plenum, New York, 1998).

[35] M. Kalff, G. Comsa, and T. Michely, Phys. Rev. Lett. **81**, 1255 (1998).

[36] Peter J. Feibelman, Phys. Rev. Lett. **81**, 168 (1998).

[37] W. T. Xu, J. G. Hou, and Z. Q. Wu, Solid State Commun. **107**, 557 (1998).

[38] B.-G. Liu, J. Wu, E. G. Wang, and Z. Y. Zhang, Phys. Rev. Lett. **83**, 1195 (1999).

[39] Zhenyu Zhang, Fang Wu, H. J. W. Zandvliet, B. Poelsema, H. Metiu, and M. G. Lagally, Phys. Rev. Lett. **74**, 3644 (1995); Z. Y. Zhang, F. Wu, and M. G. Lagally, Surf. Rev. Lett. **3**, 1449 (1996); Byung Deok Yu and Atsushi Oshiyama, Phys. Rev. Lett.

72, 3190 (1994); P. J. Bedrossian, *ibid.* **74**, 3648 (1995); B. S. Swartzentruber, A. P. Smith, and H. Jònsson, Phys. Rev. Lett. **77**, 2518 (1996).

[40] Y.-W. Mo, J. Kleiner, M. B. Webb, and M. G. Lagally, Phys. Rev. Lett. **66**, 1998 (1991); Alberto Pimpinelli, Jacques Villain, and Dietrich E. Wolf, *ibid.* **69**, 985 (1992); J. Villain, A. Pimpinelli, L. H. Tang, and D. Wolf, J. Phys. I (France) **2**, 2107 (1992).

[41] J. A. Stroscio, D. T. Pierce, and R. A. Dragoset, Phys. Rev. Lett. **70**, 3615 (1993).

[42] H. Brune, H. Röder, C. Boragno, and K. Kern, Phys. Rev. Lett. **73**, 1955 (1994).

[43] T. Ohno, Phys. Rev. Lett. **73**, 460 (1994); Thin Solid Films **272**, 331 (1996).